

Effect of uniaxial strain on anisotropic diffusion in silicon

Ming-Jer Chen and Yi-Ming Sheu

Citation: *Applied Physics Letters* **89**, 161908 (2006); doi: 10.1063/1.2362980

View online: <http://dx.doi.org/10.1063/1.2362980>

View Table of Contents: <http://scitation.aip.org/content/aip/journal/apl/89/16?ver=pdfcov>

Published by the [AIP Publishing](#)

Articles you may be interested in

[Influence of uniaxial mechanical stress on the high frequency performance of metal-oxide-semiconductor field effect transistors on \(100\) Si wafer](#)

Appl. Phys. Lett. **96**, 213515 (2010); 10.1063/1.3428793

[Effect of source/drain-extension dopant species on device performance of embedded SiGe strained p-metal oxide semiconductor field effect transistors using millisecond annealing](#)

J. Vac. Sci. Technol. B **28**, C1112 (2010); 10.1116/1.3244578

[Electron mobility in Ge and strained-Si channel ultrathin-body metal-oxide semiconductor field-effect transistors](#)

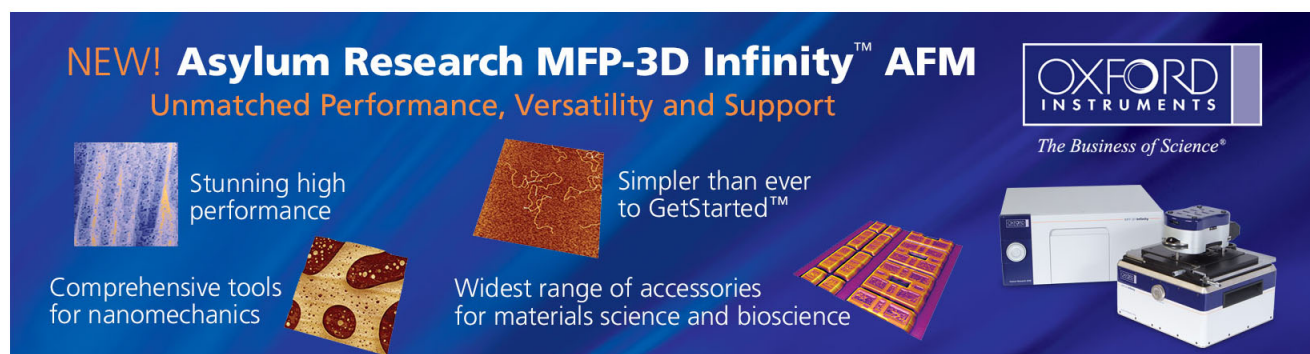
Appl. Phys. Lett. **85**, 2402 (2004); 10.1063/1.1788888

[Recrystallization, redistribution, and electrical activation of strained-silicon/Si 0.7 Ge 0.3 heterostructures with implanted arsenic](#)

J. Appl. Phys. **96**, 261 (2004); 10.1063/1.1758318

[Secondary ion mass spectrometry characterization of source/drain junctions for strained silicon channel metal-oxide-semiconductor field-effect transistors](#)

J. Vac. Sci. Technol. B **22**, 327 (2004); 10.1116/1.1640659

The advertisement features a dark blue background with white and orange text. At the top left, it reads 'NEW! Asylum Research MFP-3D Infinity™ AFM' in large white letters, followed by 'Unmatched Performance, Versatility and Support' in orange. To the right is the Oxford Instruments logo, which includes the text 'OXFORD INSTRUMENTS' and 'The Business of Science®'. Below the text are several images: a textured surface, a circular pattern, a grid of small squares, and the physical AFM instrument. Text boxes describe the instrument's capabilities: 'Stunning high performance', 'Simpler than ever to GetStarted™', 'Comprehensive tools for nanomechanics', and 'Widest range of accessories for materials science and bioscience'.

Effect of uniaxial strain on anisotropic diffusion in silicon

Ming-Jer Chen^{a)} and Yi-Ming Sheu

Department of Electronics Engineering, National Chiao Tung University, Hsin-Chu 300, Taiwan

(Received 9 June 2006; accepted 30 August 2006; published online 17 October 2006)

A physical model is directly extended from the thermodynamic framework to deal with anisotropic diffusion in uniaxially stressed silicon. With the anisotropy of the uniaxial strain induced activation energy as input, two fundamental material parameters, the activation volume and the migration strain anisotropy, can be quantitatively determined. When applied to boron, a process-device coupled simulation is performed on a *p*-type metal-oxide-semiconductor field-effect transistor undergoing uniaxial stress in a manufacturing process. The resulting material parameters have been found to be in satisfactory agreement with values presented in the literature. © 2006 American Institute of Physics. [DOI: 10.1063/1.2362980]

Strain engineering has been widely recognized as an indispensable performance booster in producing next-generation metal-oxide-semiconductor field-effect transistors (MOSFETs).^{1,2} There have been two fundamentally different methods used to achieve this goal:^{1,2} (i) biaxially strained silicon on a relaxed SiGe buffer layer and (ii) uniaxially strained silicon through the use of trench isolation, silicide, and cap layers during the manufacturing process. However, diffusion in strained silicon is essentially different from that of unstrained silicon. Thus, an understanding of strain dependent diffusion, as well as its control, is a challenging issue. So far, there have been significant studies in this direction covering a wide range of experimental findings and confirmations,³⁻⁹ atomistic calculations,¹⁰⁻¹³ physical models,¹⁰⁻¹⁶ and technology computer-aided design.¹⁷ Specifically, Cowern *et al.*⁵ experimentally revealed a linear dependence of the activation energy on strain. Within the thermodynamic framework constructed by Aziz *et al.* (see Ref. 18, which is more recent and more thorough than the earlier works cited above), the activation volume (\tilde{V}) and the anisotropy of the migration volume ($\tilde{V}_{\parallel}^m - \tilde{V}_{\perp}^m$) exist in nature. The combination of the activation energy, the activation volume, and the anisotropy of the migration volume is remarkable, as demonstrated in a physical model^{14-16,18} dedicated to both the hydrostatic pressure experiment and the in-plane biaxial stress experiment,

$$\tilde{V} + \frac{3}{2} \frac{Q'_{33\text{-biax}}}{Y_{\text{biax}}} = \pm \Omega + (\tilde{V}_{\parallel}^m - \tilde{V}_{\perp}^m), \quad (1)$$

$$\tilde{V} + \frac{3}{2} \frac{Q'_{11\text{-biax}}}{Y_{\text{biax}}} = \pm \Omega - \frac{1}{2} (\tilde{V}_{\parallel}^m - \tilde{V}_{\perp}^m), \quad (2)$$

where $Q'_{33\text{-biax}}$ is the biaxial strain induced activation energy in the direction normal to the silicon surface, Y_{biax} is the biaxial modulus, Ω is the lattice site volume, and $Q'_{11\text{-biax}}$ is the biaxial strain induced activation energy in the direction parallel to the surface.

On the other hand, in the case of uniaxial stress as encountered while fabricating the MOSFET, without the use of a relaxed SiGe buffer layer, the stress is created through the trench isolation, silicide, or cap layers in a manufacturing

process. Therefore, a straightforward extension to the uniaxial strain counterpart is essential. In this letter, one such model is derived and its linkage to the case of biaxial strain, Eqs. (1) and (2), is established. When applied to boron, a process-device coupled simulation is performed on a *p*-type MOSFET undergoing uniaxial stressing during the manufacturing process, followed by a systematic assessment of the fundamental material parameters.

According to Aziz¹⁴ and Aziz *et al.*,¹⁸ in the case of equilibrium or a quickly equilibrated point defect, the effect of stress on the dopant diffusivity in the direction normal to a (001) surface can be written as

$$\frac{D_{33}(\sigma)}{D_{33}(0)} = \exp\left(\frac{\sigma[V^f + \tilde{V}_{33}^m]}{k_B T}\right). \quad (3)$$

Here the product of the stress tensor σ and the formation strain tensor V^f is the work done against the stress field in defect formation, the product of the stress tensor σ and the migration strain tensor \tilde{V}_{33}^m is the work required for the transition in the migration path, k_B is Boltzmann's constant, and T is the diffusion temperature. The tensor V^f involves the creation or annihilation of a lattice site, followed by a relaxation process,^{14,18}

$$V^f = \pm \Omega \begin{bmatrix} 0 & & \\ & 0 & \\ & & 1 \end{bmatrix} + \frac{V^r}{3} \begin{bmatrix} 1 & & \\ & 1 & \\ & & 1 \end{bmatrix}. \quad (4)$$

The + sign denotes vacancy formation and the - sign represents interstitial formation. The relaxation volume propagates elastically to all surfaces, resulting in a change in the volume of the crystal by an amount V^r . \tilde{V}_{33}^m is expected to have the form^{14,18}

$$\tilde{V}_{33}^m = \begin{bmatrix} \tilde{V}_{\perp}^m & & \\ & \tilde{V}_{\perp}^m & \\ & & \tilde{V}_{\parallel}^m \end{bmatrix}. \quad (5)$$

In Eq. (5), \tilde{V}_{\perp}^m and \tilde{V}_{\parallel}^m , respectively, reflect the dimension changes perpendicular and parallel to the direction of the net transport when the point defect reaches its saddle point.^{14,18} Aziz further defined the activation volume as the sum of the

^{a)}Electronic mail: chenmj@faculty.nctu.edu.tw

three diagonal elements of the formation strain tensor and the migration strain tensor, as expressed by

$$\tilde{V} = \pm \Omega + V^r + 2\tilde{V}_{\perp}^m + \tilde{V}_{\parallel}^m. \quad (6)$$

It is well recognized¹² that when applying a uniaxial stress in a certain direction parallel to the silicon surface, the solid will modify its shape in order to minimize the energy of the system. In other words, the solid will deform in such a way that each surface perpendicular to the applied stress direction becomes stress-free. The underlying stress tensor therefore is

$$\sigma = \sigma_{\text{uniax}} \begin{bmatrix} 1 \\ 0 \\ 0 \end{bmatrix}. \quad (7)$$

On the basis of Hooke's law, σ_{uniax} in the linear elastic regime can be related to the uniaxial strain ϵ_{uniax} induced in the same direction: $\sigma_{\text{uniax}} = Y_{\text{uniax}} \epsilon_{\text{uniax}}$, where the uniaxial modulus $Y_{\text{uniax}} = (C_{11} - 2\nu C_{12})$ with Poisson's ratio $\nu = C_{12}/(C_{11} + C_{12})$. C_{11} and C_{12} are the elasticity constants. Analogous to previous work,⁵ the uniaxial strain induced activation energy in the direction normal to the (001) surface, $Q'_{33\text{-uniax}}$, can be linked to the underlying diffusivity,

$$\frac{D_{33}(\epsilon_{\text{uniax}})}{D_{33}(0)} = \exp\left(-\frac{Q'_{33\text{-uniax}} \epsilon_{\text{uniax}}}{k_B T}\right). \quad (8)$$

By combining Eqs. (4), (5), and (7) and equalizing Eqs. (3)–(8), one obtains $Q'_{33\text{-uniax}}/Y_{\text{uniax}} = -V^r/3 - \tilde{V}_{\perp}^m$. Again, by incorporating Eq. (6), the following expression is produced:

$$\tilde{V} + 3\frac{Q'_{33\text{-uniax}}}{Y_{\text{uniax}}} = \pm \Omega + (\tilde{V}_{\parallel}^m - \tilde{V}_{\perp}^m). \quad (9)$$

It is then a straightforward task to derive the uniaxial strain induced activation energy $Q'_{11\text{-uniax}}$ in the applied stress direction: $Q'_{11\text{-uniax}}/Y_{\text{uniax}} = -V^r/3 - \tilde{V}_{\parallel}^m$. Consequently, a similar model is achieved,

$$\tilde{V} + 3\frac{Q'_{11\text{-uniax}}}{Y_{\text{uniax}}} = \pm \Omega - 2(\tilde{V}_{\parallel}^m - \tilde{V}_{\perp}^m). \quad (10)$$

Obviously, the uniaxial strain version is closely related to its biaxial counterpart: by comparing Eqs. (1) and (9), $Q'_{33\text{-uniax}} = (Y_{\text{uniax}}/2Y_{\text{biax}})Q'_{33\text{-biax}}$ is obtained. Another relation can then be readily derived: $Q'_{11\text{-uniax}} = -(Y_{\text{uniax}}/2Y_{\text{biax}})Q'_{33\text{-biax}} + (Y_{\text{uniax}}/Y_{\text{biax}})Q'_{11\text{-biax}}$.

To produce the experimental parameters in terms of the anisotropy of the uniaxial strain induced activation energy, a uniaxial stress experiment was carried out in terms of a *p*-channel MOSFET in a state-of-the-art manufacturing process.¹⁷ The channel length was maintained at 65 nm while changing the spacing in the channel length direction between the two trench isolation sidewalls. The topside layout is detailed elsewhere.¹⁷ Under such a situation, the channel zone encounters a compressive stress from the nearby trench isolation regions in the channel length direction. The devices used are quite wide (10 μm), meaning that the strain in the channel width direction is relatively negligible. The (001) silicon surface is supposed to be stress free. This hypothesis has been validated using the sophisticated simulations detailed in Ref. 17, which revealed that in the proximity of the silicon surface, the stress in the channel length

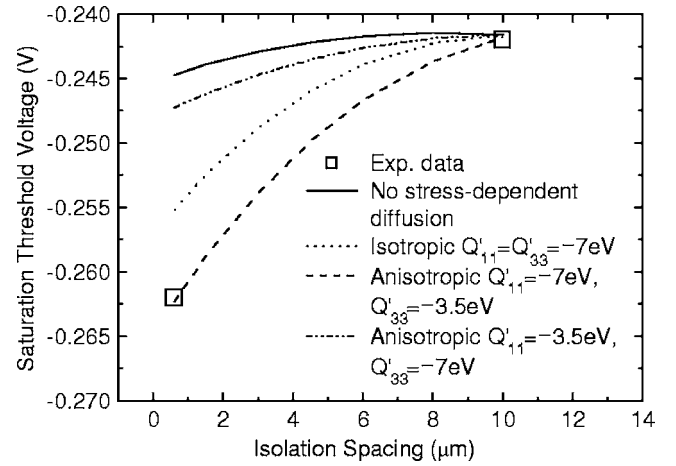


FIG. 1. Measured *p*-MOSFET saturation threshold voltage vs the spacing between the nearby trench isolation sidewalls in the channel length direction. Also shown are those (lines) from the process-device coupled simulation with and without the strain induced activation energies. The reason that the “no stress-dependent diffusion curve” is not entirely horizontal is due to dopant segregation near the edges of the source/drain regions. Specifically, the nonuniformity is caused by boron segregation occurring close to trench isolation oxide during the thermal process. Although the affected profile is not in vicinity of the MOSFET core region, a minor threshold voltage difference (~ 3 mV) between large and small active areas can still be observed, even without the stress-dependent diffusion model.

direction is much larger in magnitude than that in the direction normal to the surface. Therefore, the proposed physical model can be adequately applied. The effect of changing the spacing between the two trench isolation regions in the channel length direction is reflected in the measured saturation threshold voltage, as displayed in Fig. 1. The negative shift in the saturation threshold voltage with increasing stress (via decreasing spacing between the trench isolation regions) shown in Fig. 1 can be attributed to the retarded boron diffusion.

A two-dimensional process-device coupled simulation, as detailed in Ref. 17, was slightly modified by taking the anisotropy of the boron diffusivity into account,

$$\frac{D_{33}(\epsilon_t)}{D_{33}(0)} = \exp\left(-\frac{Q'_{33\text{-TCAD}} \epsilon_t}{k_B T}\right), \quad (11)$$

$$\frac{D_{11}(\epsilon_t)}{D_{11}(0)} = \exp\left(-\frac{Q'_{11\text{-TCAD}} \epsilon_t}{k_B T}\right). \quad (12)$$

According to the work in Ref. 17 the total strain ϵ_t is the sum of the three strain components: ϵ_{xx} in the channel length direction, ϵ_{yy} in the channel width direction, and ϵ_{zz} in the direction normal to the silicon surface. From the simulated strain distributions, $\epsilon_t \sim \epsilon_{xx}$, leading to $Q'_{33\text{-TCAD}} \approx Q'_{33\text{-uniax}}$ and $Q'_{11\text{-TCAD}} \approx Q'_{11\text{-uniax}}$. The simulated saturation threshold voltages for different values of $Q'_{33\text{-uniax}}$ and $Q'_{11\text{-uniax}}$ are plotted in Fig. 1 for comparison. The figure clearly exhibits that (i) the largest deviation occurs at $Q'_{33\text{-uniax}} = 0$ and $Q'_{11\text{-uniax}} = 0$, the case of no stress dependencies; (ii) the most accurate reproduction is achieved with the anisotropic activation energies, rather than the isotropic variety; and (iii) the anisotropy of the activation energy must be adequate, that is, $Q'_{11\text{-uniax}} = -7$ eV per unit strain and $Q'_{33\text{-uniax}} = -3.5$ eV per unit strain are more favorable than $Q'_{11\text{-uniax}} = -3.5$ eV per unit strain and $Q'_{33\text{-uniax}} = -7$ eV per unit strain.

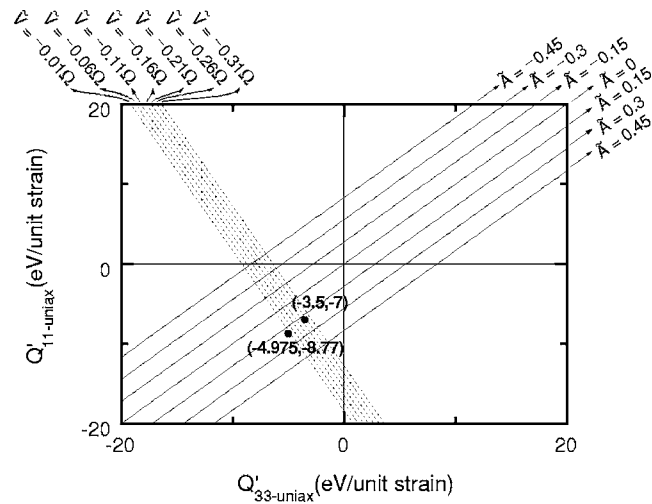


FIG. 2. Uniaxial strain induced activation energy in the applied stress direction (parallel to the silicon surface) vs that normal to the silicon surface. The lines are from Eqs. (9) and (10) for a literature range (Refs. 15, 16, and 18) of the activation volume and the migration strain anisotropy. Also plotted are the data points from the underlying experiment and the existing *ab initio* calculations (Refs. 12 and 13).

Prior to determining the fundamental material parameters, a systematic treatment, such as that indicated in Fig. 2, is demanded. In Fig. 2 a series of straight lines of $Q'_{11\text{-uniax}}$ vs $Q'_{33\text{-uniax}}$ are from Eqs. (9) and (10) for a literature range^{15,16,18} of \tilde{V} and the migration strain anisotropy \tilde{A} ($\equiv (\tilde{V}_{\parallel}^m - \tilde{V}_{\perp}^m)/\Omega$).¹⁸ In the calculation procedure, the following literature values were employed:¹⁹ (i) $C_{11}=168$ GPa and $C_{12}=65$ GPa, giving rise to $Y_{\text{uniax}}=131$ GPa and $\nu=0.28$; (ii) $\Omega=2.26 \times 10^{-23}$ cm³. The above experimental parameters are also added to the figure. From the figure a set of \tilde{V} and \tilde{A} can be clearly located around the data point. On the other hand, uncertainties exist based on a series of literature data: $\tilde{V}=-0.16 \pm 0.05$ Ω .¹⁸ Taking such uncertainties into account, Fig. 2 reveals that the data point does match the upper limit, that is, $\tilde{V}=-0.21$ Ω . The corresponding $\tilde{V}_{\parallel}^m - \tilde{V}_{\perp}^m$ in the vicinity of 0.15 Ω is determined accordingly, falling within the reasonable range.^{15,16,18} Such corroborating experimental evidence further indicates that the transient enhanced diffusion effect is relatively insignificant when compared to the long-term diffusion times in the underlying manufacturing process. Under such circumstances, the point defect is rapidly equilibrated relative to the entire diffusion time.

Finally, we quoted the existing *ab initio* calculations:^{12,13} $Q'_{11\text{-biax}}=-19.2$ eV per unit strain and $Q'_{33\text{-biax}}=-13.9$ eV per unit strain, which were transformed via the aforementioned relationship into the equivalent $Q'_{11\text{-uniax}}$ of -8.77 eV per unit strain and $Q'_{33\text{-uniax}}$ of -4.975 eV per unit strain. In this pro-

cess, the Y_{biax} used was equal to 183 GPa according to $Y_{\text{biax}}=(C_{11}+C_{12}-\nu C_{12})$ with its Poisson's ratio $\nu=2C_{12}/C_{11}$. Evidently, the two data points are quite comparable to each other, as displayed in Fig. 2.

A physical model dealing with anisotropic diffusion in uniaxially stressed silicon is derived and is quantitatively connected to the biaxial case. A process-device coupled simulation is performed on a *p*-type MOSFET undergoing uniaxial stress during the manufacturing process. A systematic treatment is conducted and the resulting fundamental material parameters are in satisfactory agreement with literature values.

This research is supported by the National Science Council of Taiwan under Contract No. NSC94-2215-E-009-005.

- ¹S. E. Thompson, M. Armstrong, C. Auth, M. Alavi, M. Buehler, R. Chau, S. Cea, T. Ghani, G. Glass, T. Hoffman, C. H. Jan, C. Kenyon, J. Klaus, K. Kuhn, Z. Ma, B. McIntyre, K. Mistry, A. Murthy, B. Obradovic, R. Nagisetty, P. Nguyen, S. Sivakumar, R. Shaheed, L. Shifren, B. Tufts, S. Tyagi, M. Bohr, and Y. El-Mansy, *IEEE Trans. Electron Devices* **51**, 1790 (2004).
- ²C. H. Ge, C. C. Lin, C. H. Ko, C. C. Huang, Y. C. Huang, B. W. Chen, B. C. Perng, C. C. Sheu, P. Y. Tsai, L. G. Yao, C. L. Wu, T. L. Lee, C. J. Chen, C. T. Wang, S. C. Lin, Y. C. Yeo, and C. Hu, *Tech. Dig. - Int. Electron Devices Meet.* **2003**, 73.
- ³N. Moriya, L. C. Feldman, H. S. Luftman, C. A. King, J. Bevk, and B. Freer, *Phys. Rev. Lett.* **71**, 883 (1993).
- ⁴P. Kuo, J. L. Hoyt, J. F. Gibbons, J. E. Turner, R. D. Jacowitz, and T. I. Kamins, *Appl. Phys. Lett.* **62**, 612 (1993).
- ⁵N. E. B. Cowern, P. C. Zalm, P. van der Sluis, D. J. Gravesteijn, and W. B. de Boer, *Phys. Rev. Lett.* **72**, 2585 (1994).
- ⁶F. H. Baumann, J. H. Huang, J. A. Rentschler, T. Y. Chang, and A. Ourmazd, *Phys. Rev. Lett.* **73**, 448 (1994).
- ⁷P. Kuo, J. L. Hoyt, J. F. Gibbons, J. E. Turner, and D. Lefforge, *Appl. Phys. Lett.* **66**, 580 (1995).
- ⁸P. Kringhoj, A. Nylandsted Larsen, and S. Y. Shirayev, *Phys. Rev. Lett.* **76**, 3372 (1996).
- ⁹N. R. Zangenberg, J. Fage-Pedersen, J. Lundsgaard Hansen, and A. Nylandsted Larsen, *J. Appl. Phys.* **94**, 3883 (2003).
- ¹⁰M. S. Daw, W. Windl, N. N. Carlson, M. Laudon, and M. P. Masquelier, *Phys. Rev. B* **64**, 045205 (2001).
- ¹¹M. Laudon, N. N. Carlson, M. P. Masquelier, M. S. Daw, and W. Windl, *Appl. Phys. Lett.* **78**, 201 (2001).
- ¹²M. Diebel, Ph.D. Dissertation, University of Washington, 2004.
- ¹³S. T. Dunham, M. Diebel, C. Ahn, and C. L. Shih, *J. Vac. Sci. Technol. B* **24**, 456 (2006).
- ¹⁴M. J. Aziz, *Appl. Phys. Lett.* **70**, 2810 (1997).
- ¹⁵Y. Zhao, M. J. Aziz, H. J. Gossmann, S. Mitha, and D. Schiferl, *Appl. Phys. Lett.* **74**, 31 (1999).
- ¹⁶Y. Zhao, M. J. Aziz, H. J. Gossmann, S. Mitha, and D. Schiferl, *Appl. Phys. Lett.* **75**, 941 (1999).
- ¹⁷Y. M. Sheu, S. J. Yang, C. C. Wang, C. S. Chang, L. P. Huang, T. Y. Huang, M. J. Chen, and C. H. Diaz, *IEEE Trans. Electron Devices* **52**, 30 (2005).
- ¹⁸M. J. Aziz, Y. Zhao, H. J. Gossmann, S. Mitha, S. P. Smith, and D. Schiferl, *Phys. Rev. B* **73**, 054101 (2006).
- ¹⁹H. F. Wolf, *Semiconductors* (Wiley, New York, 1971), p. 44.